Advances in Engineering Design Technology Vol. 2, 2020 pp. 95-107 ISSN-2682-5848

NIPES

Advances in Engineering Design Technology

Journal homepage: www.nipesjournals.org.ng

Design and Fabrication of Multi-Die Forging Machine

A.O. Jewo[a] and E. Ebojoh[b]

[a]Department of Mechanical Engineering, Petroleum Training Institute, Effurun, Delta State
[b]Department of Production Engineering, University of Benin, Benin City
email: jewo_andy@gmail.com and voke.ebojoh@uniben.edu

Article Info

Received 07 November 2020
Revised 02 December 2020
Accepted 18 December 2020
Available online 24 December 2020

Keywords:
Multi-Die, Speed Reducers, Workshop fabrication, Machine shop, washers

https://doi.org/10.37933/nipes.a/2.2020.9

https://nipesjournals.org.ng

Abstract

A multi-die forging machine was designed and fabricated successfully with a speed reducer incorporated to reduce the speed with consequent reduction in the noise and vibration level. Thorough analysis was carried out to ascertain components sizes, while special attention was also given to materials selection. Basic workshop fabrication techniques, such as cutting, turning, milling, drilling, welding was employed in the fabrication of the various parts. The machine was tested using 0.05mm and 0.5mm thick aluminum sheet and a pair of dies to produce flat washers with an average production of 120units per hour. The test results showed that the machine is capable of producing flat washers of up to 1mm thickness. The multi-die machine can be useful in machine shop and fabrication shops in urban and rural settlements.

1. Introduction

The forging process is a massive forming process, characterized by the application of a high compressive load which generates plastic strain of the billet [1]. Oviawe [2] investigated the abrasive wear distribution in a forging die under constant dimensional wear coefficient. The abrasive wear differential governing equation was used in the analysis. The finite element technique, using quadratic shape interpolation functions elements was employed to carry out the analysis over the cross-section of the die which involves discretizing the domain into finite element, analyzing this finite element, assembling the results from the analysis of the analyzed finite element, imposing the boundary conditions and finally, getting the results that represent the entire domain. Furthermore, a better way of studying abrasive wear is in terms of the specific energy, the energy equation required to remove a unit volume of material [3]. Furthermore, a developed model takes into account the deformation energy, sliding velocity and coefficient of friction of the die material and other associated parameters and proposes using the Galerkin finite element method to solve the developed model [4]. An in-depth description of repairable die defects and related die correction operations in metal extrusion was presented [5]. All major die defects are defined and classified, and their causes, preventive measures, and die correction operations are described. A brief frequency-based statistical study of die defects is also carried out to identify the most frequent die corrections. Also presented is a comparative study of different artificial intelligence techniques to map an input-output relationship of a manufacturing process and optimize the desired responses. First of all a Genetic Algorithm-Neural Network and a Taguchi-Neural Network approach are described where genetic algorithm and Taguchi are used to optimize the neural network architecture. The other techniques are support vector regression, fuzzy logic and response surface. Finally, a support vector machine approach was used to check the final product quality [6]. Further a computer-aided finite element analysis for flash-less cold forging of cup shape article was presented, where the work-piece specifications are calculated by developing mathematical relations between volumes of die cavity and work-piece. The stress deformation in the die and the punch was studied to enhance the die life [7].

2. Design consideration

Power of electric motor

The speed of rotation of the driven pulley shaft is determined using Eq. (1) [8-10].

$$N_2 = N_1 \frac{d_1}{d_2} \tag{1}$$

Formally the machines were designed to work with only two pulleys which are the motor pulley and the cam shaft pulley.

The motor pulley (driver) d_1 = 47mm = 0.047m
Camshaft pulley (driven) d_2 = 142mm = 0.142m
N_1 = Speed of electric motor = 1400 rpm

N_2 = Speed of camshaft pulley = ?

$$\frac{1400}{N_2} = \frac{142}{47}$$

Therefore; N_2 =463 rpm

Converting to linear speed

$$V = \frac{\pi d_2 N_2}{60} = 3.4\text{m/s} \tag{2}$$

This was the speed been transmitted to the camshaft hence the speed of the hammer was too fast for the design which makes the machine to be subjected to further improvement.

2.1 Determination of working speed

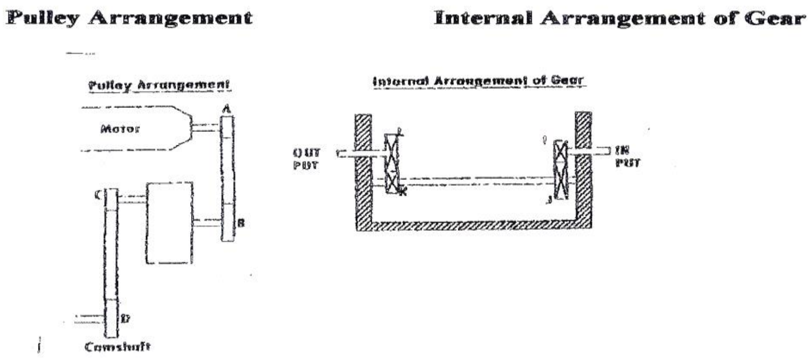

Fig. 1: Pulley and gear arrangement

(a) The first stage of speed reduction (from motor to speed reducer) which involve pulley A and Pulley B

Diameter of pulley A (Driver) d_A = 47m

Diameter of pulley B (Driven) d_B = 142mm

Speed of A, N_A = 1400rpm

Speed of B N_B is determined

$$N_B = \frac{N_A \text{ x } d_A}{d_B} = 463\text{rpm} \quad (3)$$

(b) The second stage of speed reduction (within the gears) Pulley B

$$\frac{N_C}{N_D} = \frac{d_D}{d_C} \quad (4)$$

Given

N_C=77rpm, N_d=?, dd =150mm, dc =73mm

$$N_d = \frac{N_c \text{ x } d_c}{dd} = 37\text{rpm}$$

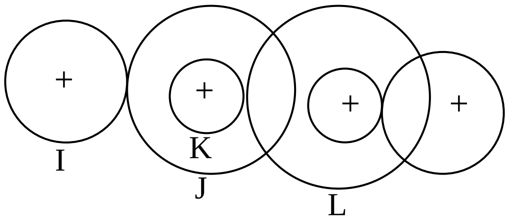

Fig. 2: Gear arrangement for second stage reduction

Numbers of teeth of I, n_i= 15, Numbers of teeth of J, n_i= 45,

Numbers of teeth of L, n_i= 66, Numbers of teeth of K, n_i= 33

where

N_F = Speed of gear F (output speed)

$$\frac{66 \text{ x } 45}{463} = \frac{15 \text{ x } 33}{N_L} = 77\text{rpm}$$

(c) The third or last stage of speed reduction (from pulley C to pulley D)

$$\frac{N_C}{N_D} = \frac{d_D}{d_C}$$

Given that

N_C = 77rpm, N_d=?, dd=150mm, dc =73mm

$$N_d = \frac{N_c \times d_c}{d_d} = 37\text{rpm} \tag{5}$$

2.2 Belt selection

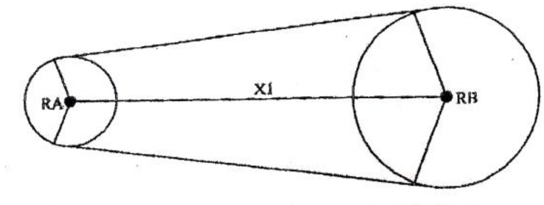

Fig 3: The length of belt (from motor to speed reducer)

$d_A=2R_A=47$mm, $d_B =2R_B =142$mm, $x_1 =270$mm

$$L_1 = \pi/2\left(d_B + d_A\right) + 2x_1 \frac{\left(d_B - d_A\right)^2}{4x_1} \tag{6}$$

:. Length of Belt $L_1 = 845$mm

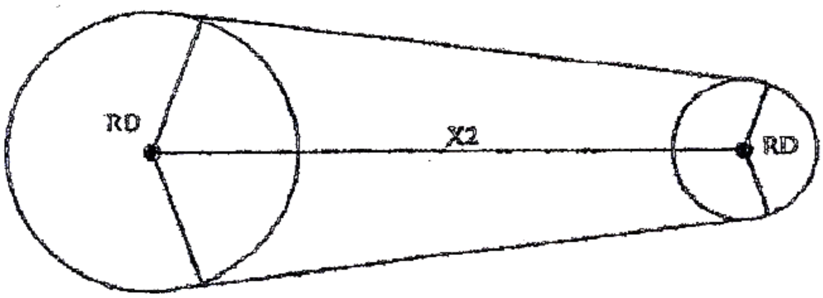

Fig. 4: Length of belt (from the speed reducer to camshaft)

$d_D = 2R_D= 150$mm, $dc=2RC = 73$mm, $X_2= 420$mm,

$$L/2 = \pi/2\left(d_D + d_C\right) + 2x_2 \frac{\left(d_D - d_C\right)^2}{4x_2}$$

. $L_2 = 1194$mm

2.3 Determination of size of belt

$c = 420$mm, $d_1=150$mm, $d_2=73$mm

$$L = 2c + 1.57\,(d_1 + d_2)= 1194\text{mm} \tag{7}$$

Adding 36mm for Type A belt

$= 1197 + 36 = 1233$mm

:. The Grade of the V belt is designed by 1233 – 50 for standard belt of inside length 1233 and a pitch length 1250.

A – 1233 – 50 / A 1233 – 145: 2494 is used in case of replacement. [8-10]

(a) Determination of the tension in the belt

From standard V – Belt dimension table according to 15:2494 – 1974 [9] the following where obtained

Thickness of belt =8.0mm, Density of belt =1250kg/m^2 Width of belt =13mm

:. Area of belt (A) $= 8 \times 13 = 104mm^2 = 10^4 \times 10^{-6}m$

For the first belt L_1

Mass of belt M = Area x Length x Density (8)

$M_1 = 0.1099kg/m$

For the Second Belt L_2

$M_2 = 0.1552kg/m$

Now using M to calculate For T_1 and T_2 and the power transmitted from Eq. 8

$$T_c = MV^2 \quad (9)$$

where

$$V_1 = \frac{\pi dp \;\; x \;\; N_C}{60} = \frac{22 \, x \, 0.047 \;\; x \;\; 1400}{7 \;\; x \;\; 60} = 3.4m/s$$

:. $T_{cl} = 0.1099 \times 3.4^2 = 1.27N$

Maximum tension of the belt $T = \sigma \times A$, (10)

where

σ = the allowable tensile stress.

$T = \sigma \times 104 \times 10^{-6}$

The ultimate strength of leather belt varies from 21 to 35 MPa and factor of safety may be taken as 8 to 10. However, the wear life of a belt is more important than actual strength. It has been shown by experience that under average condition an allowable stress of 2.8 MPa or less of 1.75 MPa may be expected to give a belt life of about 15 years [8-10].
So, a factor of safe of 8 was chosen for 22Mpa

$$\text{Allowable tensile stress} = \frac{\text{Ultimate tensile stress}}{\text{Factors of safety}} \quad (11)$$

:. $\sigma = 2.75Mpa$

$T = 286N$

But tension on the tight side $T_1 = T - T_c$ (12)

:. $T_1 = 286N - 1.27$

$= 284.7N$

But $\frac{T_1}{T_2} = e^{\mu\theta\cos}$ (13)

Where μ = 0.25 (standard value)

Groove angle

β = 38/2 (standard value)

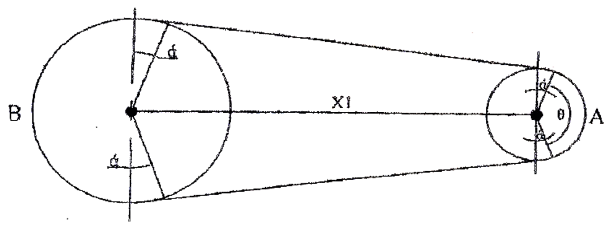

Fig. 5: Angle of wrap of pulley A

From the Fig. 5

$$\text{Sin } \alpha = \frac{d_B - d_A}{2x_1} \quad (14)$$

$$\text{Sin}\alpha = \frac{0.142 - 0.047}{2 \times 0.27} = \frac{0.095}{0.54}$$

$$\alpha = \text{Sin}^{-1}\ 0.1759 = 10^0$$

Angle of wrap on the smaller pulley (Motor pulley)

$$\theta = 180 - 20 = 160^0 = 2.8\text{rad}$$

$$\frac{T_1}{T_2} = e^{0.25 \times 2.8 \times \operatorname{cosec} 38/2}$$

$$\frac{284.7}{8.6} = 33.1\text{N}$$

Power transmitted by the first belt

$$P = (T_1 - T_2)\ V \quad (15)$$

$$P_1 = 0.855\text{kW}$$

Now, using M_2 to calculate for T_1, T_2 and power transmitted by the second belt

$$T_{c2} = M_2\ V^2$$

$$V_2 = \frac{\pi d c N_c}{60} = 0.29\text{m/s}$$

$$T_{c2} = 0.1552 \times 0.292 = 0.013\text{N}$$

Maximum tension of belt

$T = \alpha \;\; x \;\; A$

$T = 2.75 \text{ x } 10^6 \text{ x } 104 \text{ x } 10^{-6}$

$T = 286N$

Tension on the side T_1 = 286 - 0.013

$T_1 = 285.99N$

But $\frac{T_1}{T_2} = e^{\mu\theta\cos}$

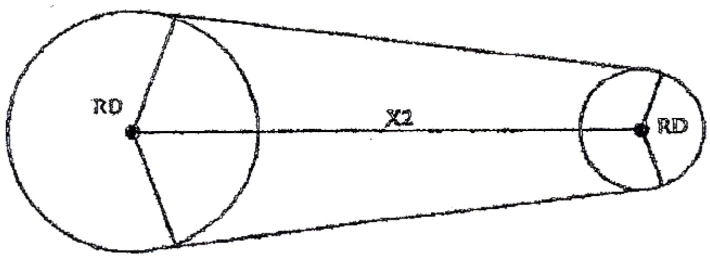

Fig. 6: Angle of wrap of pulley C

Using Sin σ $= \frac{dD}{2 \text{ x } 2} = \frac{150 \text{ x } 73}{2 \text{ x } 420} = 0.092$

Sin σ $= \sin^{-1} 0.092 = 5.3^0$

Angle of wrap $\theta = 180 - 2\alpha = 180 - 2 \text{ x } 5.3$ (16)

$\theta = 169.4 = \frac{169.4 \text{ x } 22}{7 \text{ x} 180} = 2.95\text{rad}$

$\therefore = \frac{285.99}{T_2} = e^{0.25 \text{ x } 2.95 \text{x } 3.07}$

$= \frac{285.99}{T_2} = e^{0.26} = 9.58$

$T_2 \quad \frac{285.99}{9.58} = 29.9N$

Power transmitted by the second belt

Using Eq. 15

$P_2 = (285.99 - 29.9)\, 0.29 = 74.3W$

$P_2 = 0.074kW$

2.4 Bearing design

According to SKF Bearing Catalogue (2012), the basic dynamic load can be deduced from Eq. 17

$$F_e = (XCrF_r + CtF_{tr})S.F \tag{17}$$

Where, rotational factor =1 (inner raceway), radial factor = 1, thrust load =0 (Since the bearing is not carrying axial load), safety or service factor = 1.2 (taken).
Eq. 18 reduces to

$$F_e = (XCrF_r)S.F$$

From SKF bearing Catalogue (2012), basic life of the bearing, L_{10} is given in Eq.18

$$L10 = \frac{60 \times Li_{be} \times N_2}{10^{6}} \tag{18}$$

Life of the bearing = 20,000

$$L10 = \frac{60 \times 20000 \times 933.33}{10^{6}} = 1120\, millions\ of\ revolution$$

The basic dynamic load is given by Eq. (19)

$$C = (L10)^{1/k} F_e \tag{19}$$

Where, k = 3 (Ball bearing).

$$C = (1120)^{1/3} \times F_e \tag{20}$$

The forces acting on the driven shaft are shown in Fig. 7,

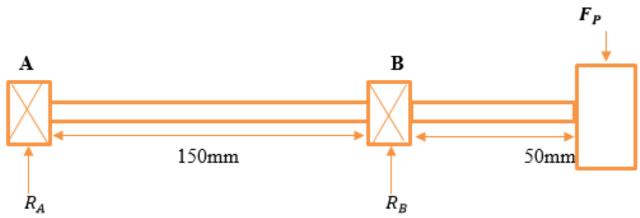

Fig. 7: Forces acting on the driven shaft

Force acting on the driven pulley is given by Eq. (21)

$$F_p = \frac{Tr_{bt}}{d_2} \tag{21}$$

$$F_p = \frac{20.7902}{0.75} = 277.2021N$$

$$R_A + R_B = F_p \tag{22}$$

$$R_A + R_B = 277.2021N$$

Upward reaction (Forces) = Downward reaction (Forces)
Taking moment about point A,

$$277.2021(150 + 50) = R_B \times 150$$

$$R_B = 369.6028N$$

$$R_A = 277.2021 - 369.6028$$

$$R_A = -92.4N$$

$$F_e = (1 \times 1 \times 92.4)1.2 = 110.88N$$

$$C = (1120)^{1/3} \times 110.88 = 1151.487N$$

A deep groove ball bearing designation 61804 was selected for bearings A and B from the SKF Bearing Catalogue for the following reasons: Cost, maintenance and availability

Determination of shaft diameter

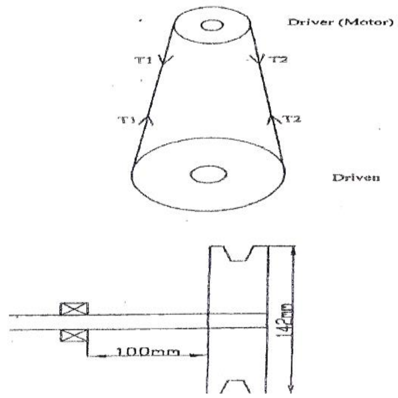

Fig. 8: Shaft pulley arrangement

T_1 = 284.7N

T_2 = 33.1N

Torque transmitted by the shaft

$$T = (T_1 - T_2) R = (284.7 - 33.1)\ 142/2 \times 1000 \tag{23}$$

$$T = 2516 \text{ X } 0.071 = 17.86Nm$$

Neglecting weight of shaft, total vertical load acting on the pulley

$$W = T_1 + T_2 \tag{24}$$

$$= 284.7 + 33.1 = 317.8N$$

Bending moment M = W x L

Where L = 100mm

$$M = 317.8 \times 100 = 31790N^{-}mm$$

$$\text{Equivalent twisting moment } T_c = \sqrt{M^2 + T^2} = \frac{\pi}{16} \times \tau \times d^3 \tag{25}$$

$$T_e = \sqrt{31780^2 + 17860^2}$$

$$\sqrt{1009968400 + 13897600}$$

$$T_e = 26286.7N^{-}mm$$

$$\text{Also, } T_e = \frac{\pi}{16} \times \tau \times d^3 \text{(from Eq. 25)} \tag{26}$$

According to America Society of Mechanical Engineering (ASME) code for the design of transmission shaft the maximum permissible shear stress may be taken as

(a) 56MPa for shaft without allowance for key way

(b) 42MPa for shaft with allowance for key way

= $42N/mm^2$

$$\therefore \quad 26286.7 = \frac{22}{7 \times 16} \times 40 \times d^3$$

$$d^3 = \frac{26286.1 \times 7 \times 10}{22 \times 42} = 3186.3$$

$$d = 15m$$

:. Diameter of shaft = 20mm (chosen)

According to the calculated shaft diameter, the shaft bearing was selected [8-10]

Shaft diameter d = 20mm

From Table [8-10]

22mm diameter of shafts was chosen because it is the closest to 20mm shaft.

Width of Key W = 8mm

Thickness t = 7mm

Using Eq. 27 from chapter two

$$\text{Length of key } L = 1.571d \tag{27}$$

$$L = 1.571\,(20)$$

$$= 31.42$$

$$= 32mm$$

3. Fabrication of the machine

The fabrication was done at Petroleum Training Institute Mechanical Machine and Fabrication workshop Effurun. The materials used were sourced for locally after designing for the various components. Mild Steel contains 0.05 to 0.30% Carbon; Medium Carbon Steel contains 0.30 to 0.60% Carbon. The manufacturing processes employed in the fabrication/assembling of the machine include drilling, cutting, filing, painting, etc..

Table 1: Materials selected for components parts of the forging machine.

S/N	**Components Part**	**Materials Selected**
1	Gear	Medium carbon steel
2	Shaft	Medium carbon steel
3	Pulley	Mild steel
4	Belt	Impregnate rubber

5	Gear/Speed –Reducer Box	Mild steel
6	Bearing	Alloy steel
7	Die	Alloy steel

Table 2: Component parts of material selected and process used in manufacturing

S/N	**Component Parts**	**Material Selecting**	**Process**
I	Gear .	Medium Carbon Steel	Cutting, turning Milling, Drilling and heat treatment
2.	Shaft	Medium Carbon Steel	Turning, Milling and Heat Treatment
3.	Pulley	Mild Steel	Turning, Drilling
4.	Bushing	Mild Steel	Cutting and Grinding
5.	Belt	Impregnate Rubber	Standard
6	Gear/Speed-Reducer Box	Mild Steel	Cutting, Grinding, Drilling welding
7.	Bearing	Alloy steel	Standard

3.1 Construction and assembly

The Multi-Die Forging Machine was designed and constructed based on material availability. It is rectangular in shape with dimension of (750 x 394 x 810) mm; this is because we are designing for a small and portable size forging machine.

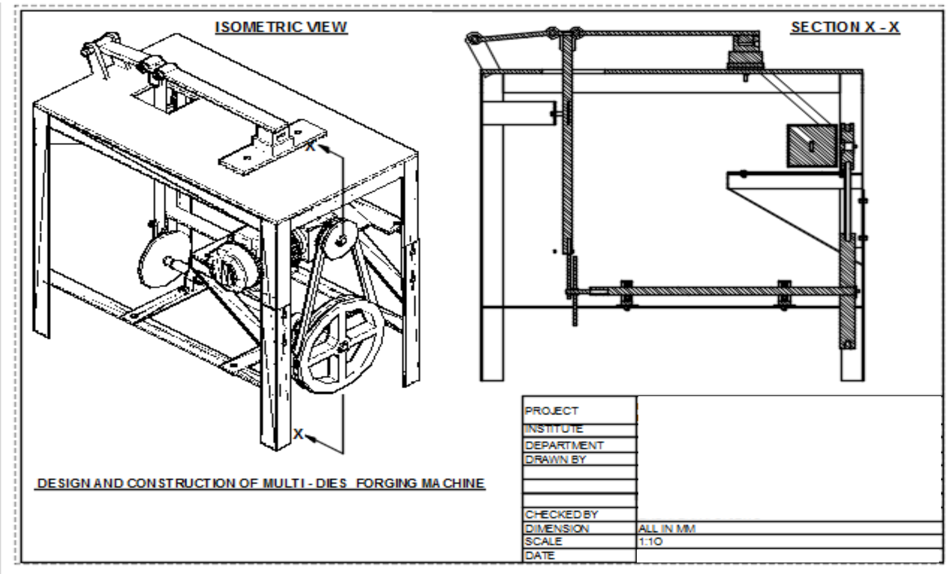

Fig. 1: Pictorial view of multi-die forging machine

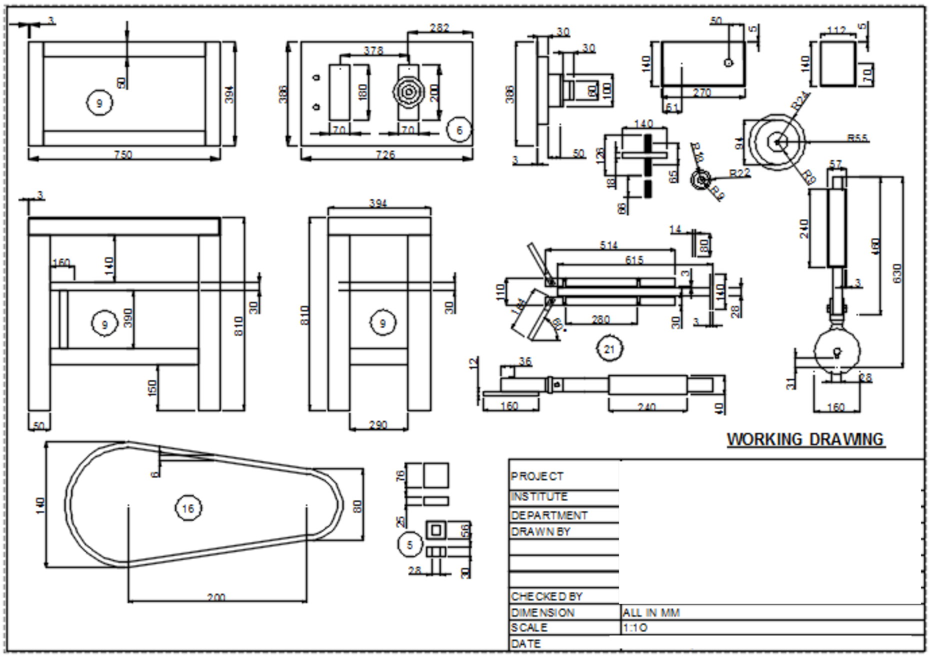

Fig. 2: Working drawing of multi-die forging machine

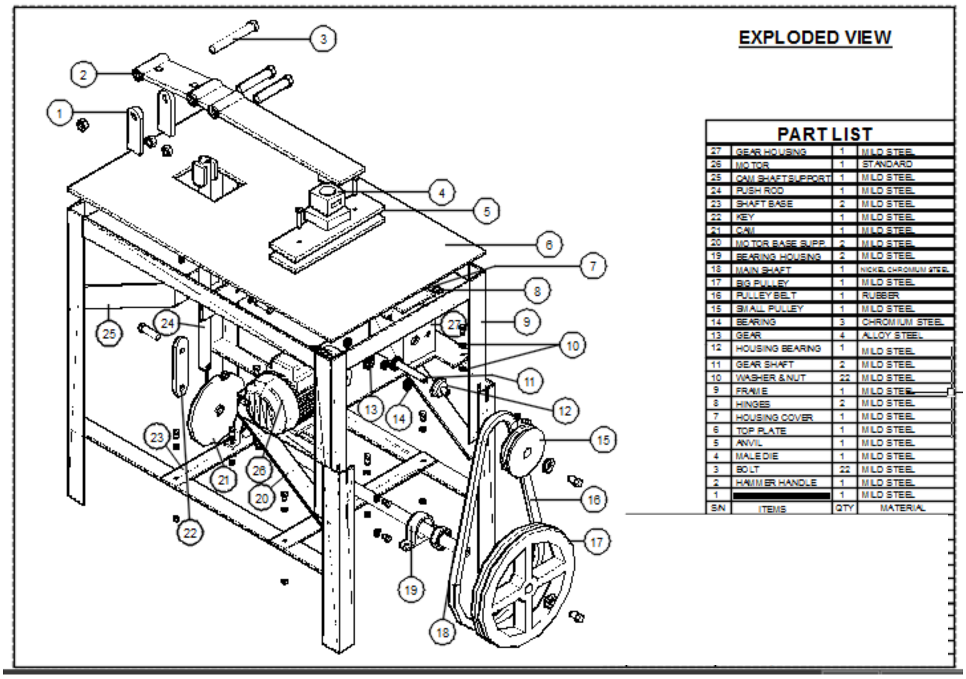

Fig. 3: Pictorial view of multi-die forging machine

3.2 Cost analysis

From the design and fabrication stage, the cost of manufacture is of high priority based on labor and overhead cost. Hence minimization of cost is a target. The choice of locally available materials was sought after to make the machine affordable for small and medium scale industries. From the forgoing the cost of production is N110,000.00

3.3 Performance evaluation

The machine was tested using 0.05mm and 0.5mm thick aluminum sheet and a pair of dies to produce flat washers. The test results showed that the machine is capable of producing flat washers of up to 0.5mm thickness with an average production of 120units per hour.

4. Conclusion

The multi-die forging machine is designed to be simple with special consideration to cost of production and materials used and to enhance the stroke output by selecting appropriate power transmission system. The test result shows that the machine is capable of forging sheet metals of up to 0.5mm thickness with appropriate dies while special consideration can be given to gasket production.

It is expected that with the low cost of production, every small and medium enterprise can afford the machine to carry out the desired function.

Reference

[1] Altan T. (2005), Cold and Hot Forging: Fundamentals and Applications. ASM International, 2005
[2] Oviawe C.I, Akpobi J.A. and Oviawe O. (2018), Analysis and Prediction of Die Wear In Hot Forging Operation. The Journal of the Nigerian Institution of Production Engineers Vol. 22, pp.216-224
[3] Shaw M.C. Metal cutting principles. Oxford Science Publishers 2005, 170-175
[4] Ebojoh E. and Amgbari C. (2018) Proposed Model for Predicting Abrasive Wear in Hot Forging Dies. International Journal of Advanced Engineering and Technology. Volume 2; Issue 2; pp 72-73
[5] Sayyad Z. Q, Tasneem P. and Josiah C. C. (2018), Die Defects and Die Corrections in Metal Extrusion. Metals 8, 380; doi:10.3390/met8060380
[6] Claudio C., Teresa C., Giuseppina A., Luigi F., Roberto M. (2015), Design of a High Performance Predictive Tool for Forging Operation. 9th CIRP Conference on Intelligent Computation in Manufacturing Engineering. Procedia CIRP 33 (2015) 173 – 178
[7] Khaleed H.M.T., Addas M.F., Mujeebu M.A., Abdullah A. A, Irfan A.B., Quadir G.A., Salman A.N.J, Khan T.M.Y., Sarfaraz K. (2014) Flash-less Cold Forging of Cup-shaped Object and Stress Analysis of Forging Die using FEM Simulation and Experiment. Australian Journal of Basic and Applied Sciences, 8(24) pp. 401-410
[8] Khurmi, R. S. and Gupta, J. K. (2005) "Machine Design" Eurasin Publishing House (pvt) Ltd, Ram Nagar New Delhi.
[9] Khurmi, R. S. and Gupta, J. K. (2006) "Machine Design 14th Revised Edition" Eurasin Publishing House (PVT) Ltd, Ram Nagar New Delhi.
[10] Khurmi, R. S. (2006) "Strength of Material" S. Chand and Company (PVT) Ltd, Ram Nagar New Delhi.